Electrochemical Impedance Spectroscopy (EIS) of NaCl-Saturated Sandy Soil at Sub-zero Temperatures

Zhiwei Chen, Pengju Han[*], Bin He*[*], Funan Sun, Xiangling Bai, Xingyi Wang, Tiantian Guo and Xiaoyuan Wang*

College of Civil Engineering, Taiyuan University of Technology, Taiyuan, 030024, China
[*]E-mail: 13834569544@163.com, hebin@tyut.edu.com

In this paper, NaCl-saturated sandy soil at sub-zero temperatures was studied with electrochemical impedance spectroscopy (EIS). By considering the microstructure of the NaCl-saturated sandy soil, an equivalent circuit (EC) model (R_{CCP} (C_{IP} (C_{DCP} R_{DCP}))) is proposed on the basis of three kinds of conductive paths (continuous conductive paths (CCPs), discontinuous conductive paths (DCPs), and insulating paths (IPs). The correctness and suitability of the EC model are indicated by the small values of the chi-square statistic and fitting errors. The four circuit elements in this equivalent circuit model are associated with soil components, and the freezing of water to ice is the main cause of changes in their values. The fitting results obtained by this equivalent circuit model suggest that the values of the R_{CCP} and R_{DCP} increase exponentially with decreasing temperature. There is an obvious change in the trends for the values of the C_{DCP} and C_{IP} that depends on the freezing temperature. The proposed EC model can successfully explain the EIS results and help provide a better understanding of the microstructure of frozen soil. In addition, the model can be applied in other types of frozen soils and support studies of the corrosion of steel buried in soils at sub-zero temperatures, which can further broaden the application of EIS.

1. INTRODUCTION

NaCl-saturated sandy soil are common in some provinces in northern China, including Xinjiang, Inner Mongolia, Shanxi, etc. In these locations, the temperature is below 0 ℃ in the winter, and the temperature can even reach -20 ℃ [1]. Furthermore, there are many oil and gas pipelines buried in these areas. The microstructure of saline sandy soil saturated with NaCl at sub-zero temperatures, especially below the freezing temperature of the soil, has significant effects on the

Int. J. Electrochem. Sci., 16 **(2021)** Article ID: 210914

2

mechanical strength and corrosion of pipeline steel.

Electrochemical impedance spectroscopy (EIS) has proven to be an effective and sensitive tool to study the corrosion of steel [2-5] and the microstructure of porous media, such as concrete [6, 7] and soils [8, 9]. EC models based on the microstructure are considered a powerful approach to simulate and interpret EIS results. Song [6] proposed an equivalent circuit model for concrete based on the microstructure characterization, which contains meaningful parameters that can explain experimental phenomena. Han et al. [8] proposed an equivalent circuit model based on three different kinds of conductive paths related to the microstructure and composition of the soil. Many papers can be found in the literature describing EC models for soils that are used to study corrosion of steel [3, 5, 10-14]. However, the above studies were almost always carried out at room temperature, and the above EC models did not consider the influence of temperature. Some of the pore water in soil freezes into ice below the freezing temperature, and the conductive paths change. In this case, the EC models mentioned above may not be applicable for soils at sub-zero temperatures.

Therefore, it is important to study the electrochemical impedance spectroscopy (EIS) of soils at sub-zero temperatures. The present study focuses on the application of EIS to study sandy NaCl-saturated sandy soil at sub-zero temperatures. The purpose of this paper is to propose an EC model containing meaningful parameters based on the soil microstructure, which can support the interpretation of EIS results and studies of the corrosion of steel in soils at sub-zero temperatures.

2. MATERIALS AND EXPERIMENTS

2.1. Preparation of soil samples

Sandy soil, sodium chloride (certified AR for analysis) and deionized water were used to prepare NaCl-saturated sandy soil. The sandy soil used in this study was produced by Xiamen ISO Standard Sand Co. Ltd, China. The chemical composition and percentage composition are listed in Table 1.

Table 1. The chemical composition of the ISO standard sand

Components	SiO_2	Fe_2O_3	Al_2O_3	CaO	MgO	Others
Contents/%	98.7	0.1	0.7	0.1	0.1	0.3

To control the NaCl content more accurately, the ISO standard sand was washed several times with deionized water until the measured NaCl content was less than 0.1%. Next, the soil sample was dried at 105 °C for 12 hours. Then, sodium chloride was dissolved in deionized water. Each soil sample (510 g) was mixed with a NaCl solution. Solutions with different NaCl concentrations were used. The prepared NaCl-saturated sandy soil samples contained 18% water and 1%, 2%, 3% or 5% NaCl (ratio of NaCl mass to dry soil mass).

Table 2. The basic physical properties of the ISO standard sand

Density (d_s)	Minimum dry density (ρ_{dmin})	Maximum dry density (ρ_{dmax})	Minimum void ratio (e_{min})	Maximum void ratio (e_{max})
2.66 g/cm^3	1.56 g/cm^3	1.86 g/cm^3	0.430	0.705

The basic physical properties of the ISO standard sand are shown in

Table 2. In this study, the water content (ω) and relative density (D_r) of the soil samples are 18% and 0.5, respectively. From the basic physical properties in Table 2 and Equation (1), the void ratio (e) and dry density (ρ_d) can be obtained as 0.568 and 1.70 g/cm^3, respectively.

$$D_r = \frac{e_{max} - e}{e_{max} - e_{min}} = \frac{\rho_{dmax}(\rho_d - \rho_{dmin})}{\rho_d(\rho_{dmax} - \rho_{dmin})} \qquad (1)$$

Soil samples were sealed in containers for 24 hours so that the water and NaCl could be evenly distributed. Each prepared soil sample was placed in a 7.0 cm × 7.0 cm × 7.0 cm insulated plastic mould and compacted. The height of each soil sample was 6.0 cm to control the dry density (D_r) at 1.70 g/cm^3. A temperature sensor with an accuracy of 0.01 °C was embedded in the centre of the soil sample to record the cooling curve and detect the real-time temperature. A waterproof breathable membrane covered the plastic mould to ensure that the water content of the soil sample remained unchanged during the test. The soil sample testing device is shown in Figure 1.
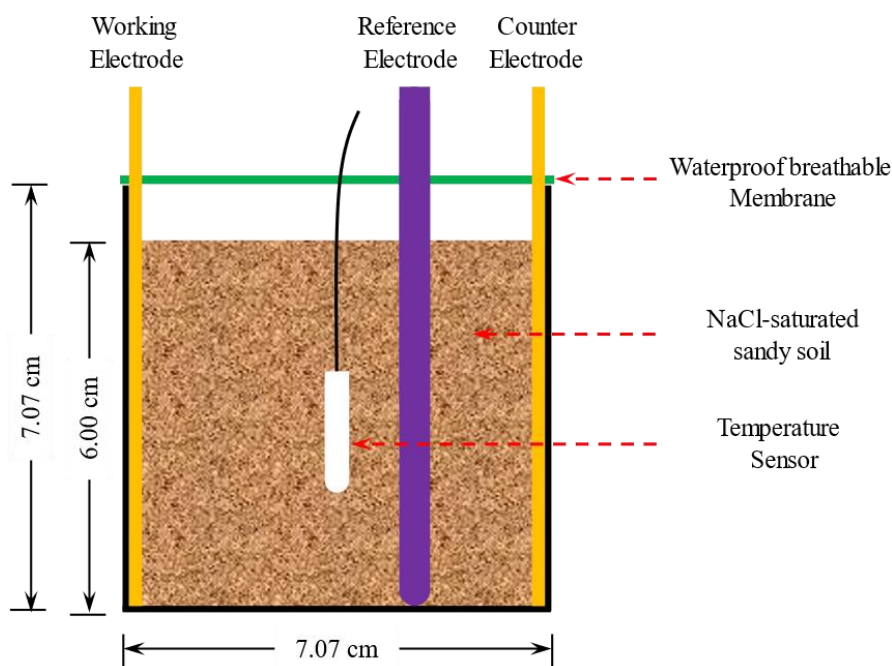

Figure 1. Soil sample testing device

2.2. Testing instruments and methods

The temperature was controlled with a constant temperature bath (model DHC-2005-A produced by Hangzhou Qiwei Instrument Co., LTD, China), and the temperature control accuracy was ± 0.1 °C. Considering the solubility of NaCl and ensuring that the temperature of each sample was consistent before cooling, each soil sample was first kept at 20 °C for 3 hours. Then, the temperature of the bath was lowered to different test temperatures. The test temperature range was from 0 °C to -20 °C in -5 °C steps, i.e., 0 °C, - 5 °C, -10 °C, -15 °C and -20 °C. When the sample temperature reached the test temperature, EIS measurements were performed. A CS350H electrochemical workstation was used to measure the EIS spectra. When the open circuit potential (OCP) was stable, EIS were acquired over the frequency range of $10^{-2} \sim 10^{5}$ Hz using a sinusoidal voltage signal with a 10 mV amplitude [15].

The EIS measurements were performed using a classic three-electrode system, which included a working electrode (WE), a counter electrode (CE) and a reference electrode (RE). Copper sheets, cleaned and polished, were used as electrodes. The working electrode (WE) and counter electrode (CE) were placed on opposite sides of the soil sample, and the reference electrode (RE) was inserted into the soil sample (see Figure 1). During the test, a high-precision temperature sensor embedded in the soil was used to measure the temperature in real time, and the data were transferred to the computer at intervals of 10 s.

3. RESULTS AND ANALYSIS

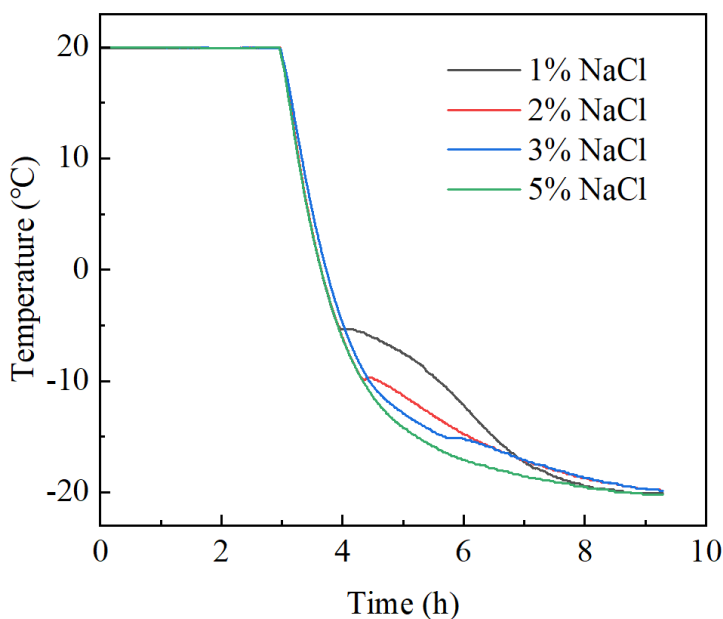*3.1. Cooling curves and freezing temperatures of the soil samples*

Figure 2. Cooling curves of NaCl-saturated sandy soil during the cooling process

The water in the soil freezes and condenses into ice at sub-zero temperatures. Unlike soil above 0 °C, ice forms in the soil at sub-zero temperatures [16]. This changes the structural characteristics of soil; therefore, it is of great importance to determine whether there is ice in the soil. The temperature determines whether the liquid water in the soil turns into ice. The ice formation process includes the nucleation and growth of ice crystals. The freezing of water in soil generally includes four stages: (1) supercooling, (2) a step-like increase in temperature, (3) constant temperature, and (4) a decrease in temperature. The temperature at the third stage is taken as the freezing temperature [17]. Figure 2 presents the curves of the temperature of NaCl-saturated sandy soil during the cooling process. As the NaCl content increases, the freezing temperature gradually decreases. In addition, due to the limitation of the test temperature range (from 0 °C to -20 °C), the freezing temperature of the NaCl-saturated sandy soil sample with 5% NaCl was not measured because this soil sample did not freeze within the test temperature range. The freezing temperatures of NaCl-saturated sandy soil with different NaCl contents are listed in Table 3.
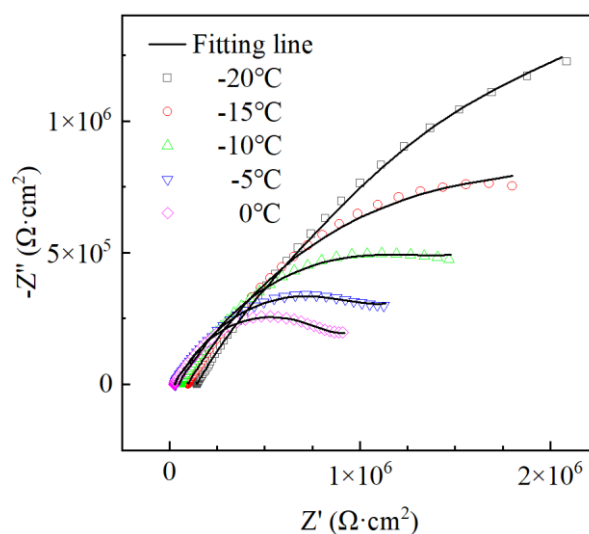
Table 3. Freezing temperatures of NaCl-saturated sandy soil with different NaCl contents

NaCl content	1%	2%	3%	5%
Freezing temperature/°C	-4.8	-8.9	-13.8	—

3.2. Analysis of Nyquist plots and Bode plots

(a) NaCl content = 1%   (b) NaCl content = 2%
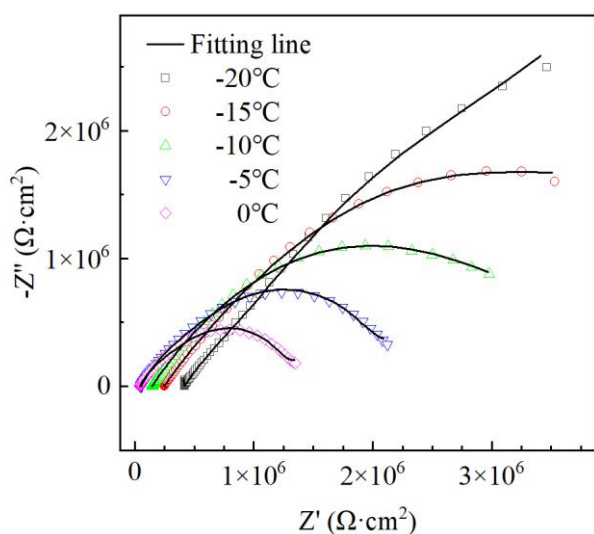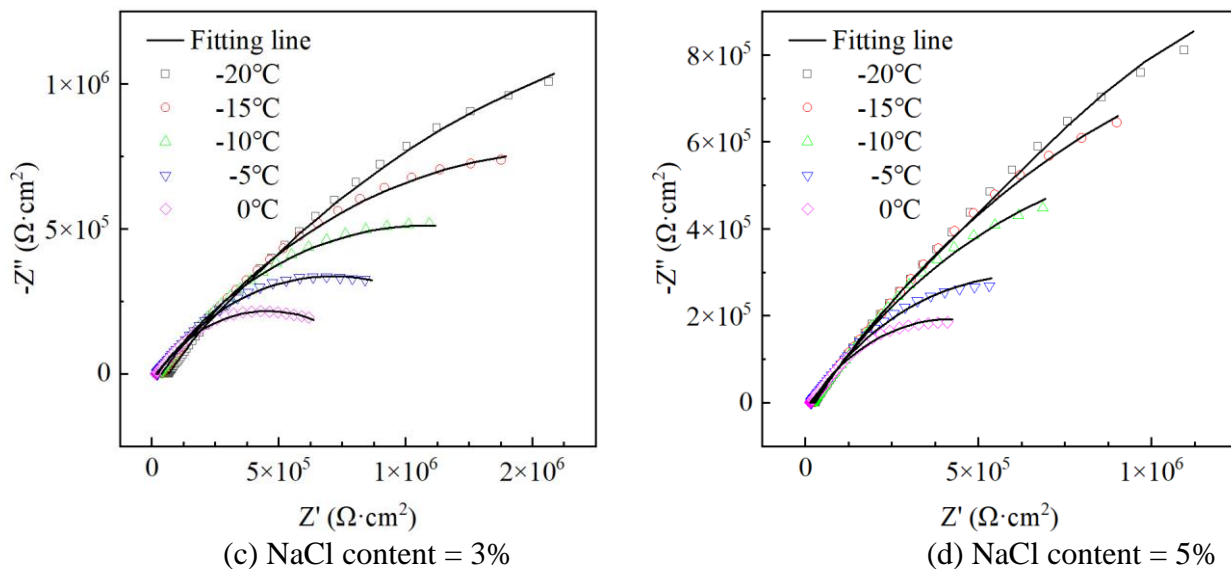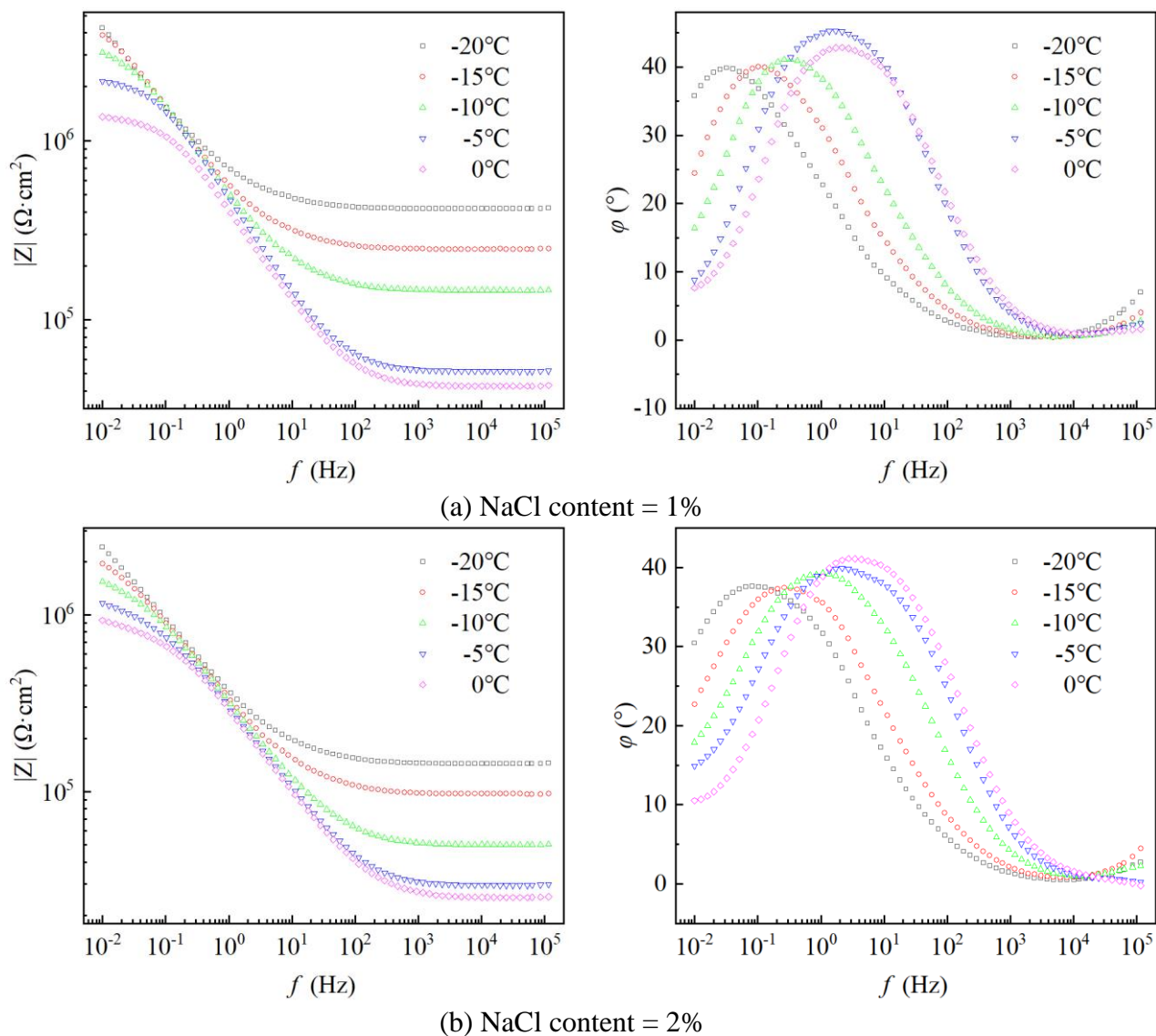
(c) NaCl content = 3%   (d) NaCl content = 5%

Figure 3. Nyquist plots of NaCl-saturated sandy soil with various NaCl contents

(a) NaCl content = 1%

(b) NaCl content = 2%

(c) NaCl content = 3%
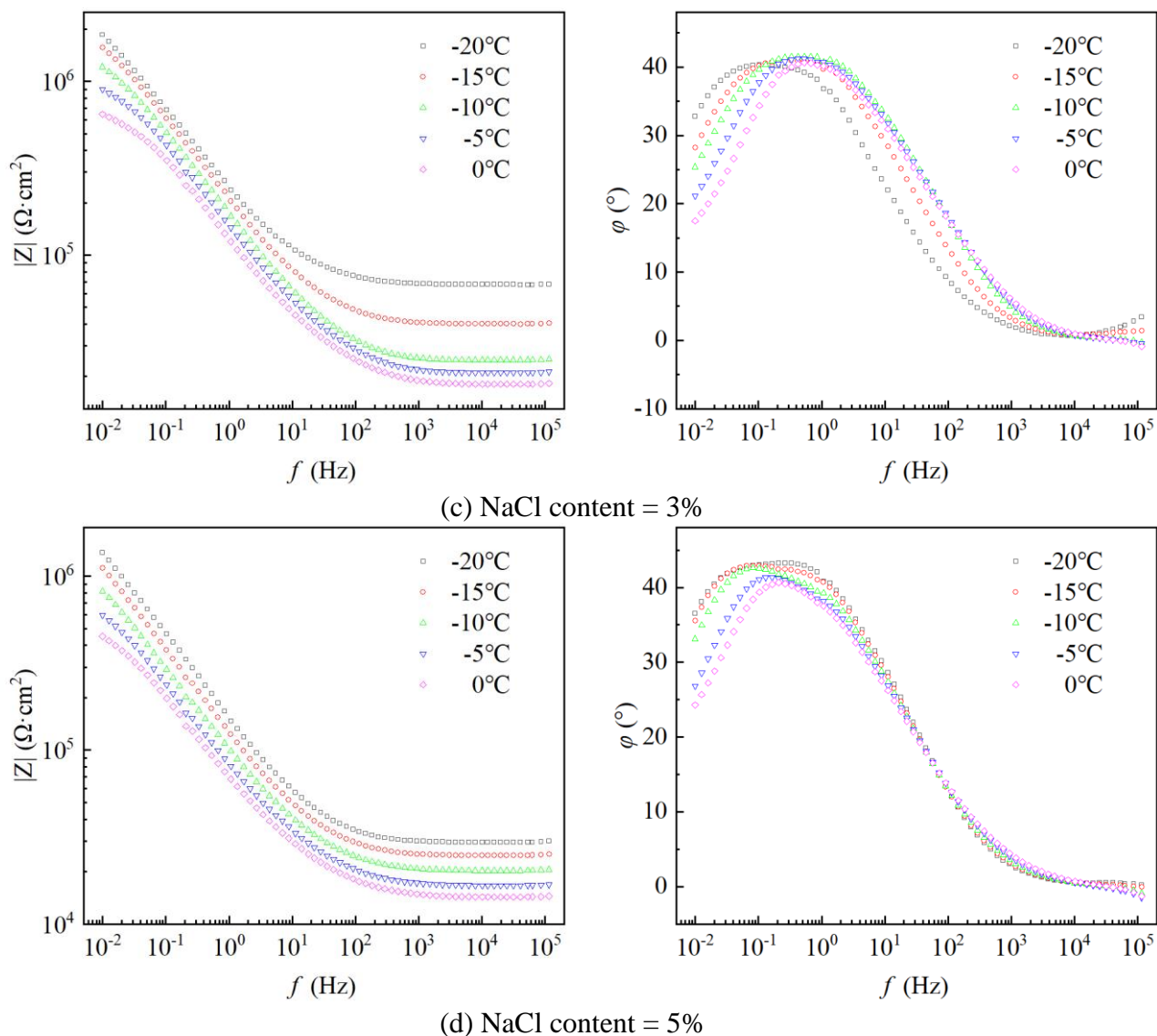

(d) NaCl content = 5%

Figure 4. Bode plots of NaCl-saturated sandy soil with various NaCl contents

The results of EIS measurements are presented as Nyquist plots (Figure 3) and Bode plots (Figure 4). All the Nyquist plots show a clear capacitive reactance loop. At a given NaCl content, the radius of the capacitive reactance loop increases with increasing temperature. Furthermore, when the NaCl content of the soil sample is higher, the radius of the capacitive reactance loop is smaller at the same temperature. The radius of the capacitive reactance loop is related to the charge transfer rate [18].

In the Bode magnitude plots, at a given NaCl content, the impedance modulus increases with increasing temperature, and the impedance modulus abruptly increases when the soil sample is cooled below the freezing temperature. In the Bode phase angle plots, the large phase angle peak could indicate the interaction of at least two time constants [19]. Phase angles approaching 90° suggest that the electrode surface is smooth and dense [20, 21]. The maximum phase angle values in this study were between 25° and 45°, confirming that the electrode surface was rough, and pore structure was present at the contact interface between the electrode and soil, which is related to the porosity of the soil. For these five groups of soil samples with different salinities, the peak value of the maximum

phase angle decreases and shifts to lower frequencies when the temperature is below the freezing temperature. This shows that the decrease in temperature causes the chemical reaction rate to slow down.

3.3. Equivalent circuit model

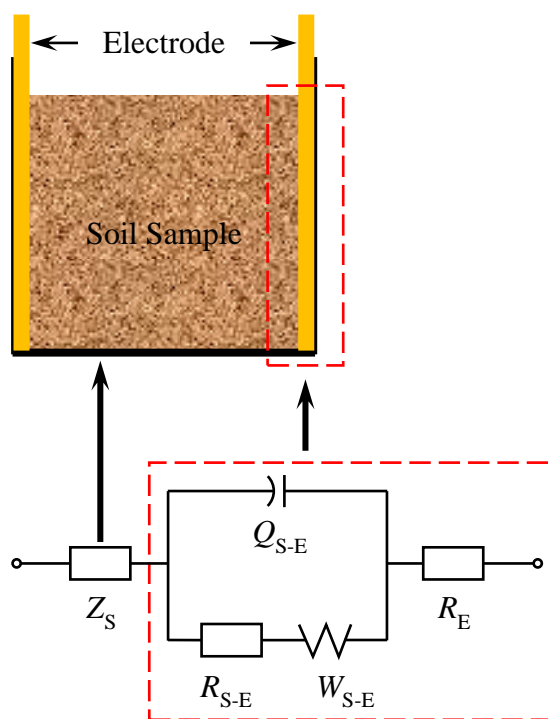### 3.3.1. Equivalent circuit model in this study

Figure 5. Schematic representation of the relevant equivalent circuit model used in this study. Z_S, the impedance of the soil sample; Q_{S-E}, a constant phase element between the soil sample and electrode; R_{S-E}, the resistance between the soil sample and electrode; W_{S-E}, the Warburg impedance between the soil sample and electrode; and R_E, the resistance of the electrode.

Figure 5 shows the schematic representation of the relevant equivalent circuit model in this study. The EC model can be described as Z_S (Q_{S-E} (R_{S-E} W_{S-E})) R_E. The element Z_S, which is introduced in the next section of this paper, is the impedance of the soil sample. All the electrodes used in this study are solid. At these solid electrodes, the double-layer capacitance often displays a certain frequency dispersion. Such behaviour cannot be modelled by a simple capacitance element. A constant phase element (CPE) is usually used to explain such behaviour [22]. Therefore, between the soil sample and electrode, Q_{S-E} is a constant phase element (CPE) used to replace the electrode double-layer capacitance. It can be defined by:

$$Q_{S-E} = [Y_0 (j\omega)^n]^{-1} \qquad (2)$$

where Y_0 is the magnitude of the CPE with units of $S \cdot sec^n \cdot cm^{-2}$; j is the imaginary unit with $j = \sqrt{-1}$; ω is the angular frequency with $\omega = 2\pi f$ where f is the voltage signal frequency; and n is

the exponent of Q with values between 0 and 1 [23, 24].

$R_{\text{S-E}}$ is the resistance between the soil sample and electrode, referred to as the charge transfer resistance in many studies. $W_{\text{S-E}}$ is the Warburg impedance between the soil sample and electrode. R_{E} represents the resistance of the electrode, which can be ignored due to its small value.

The second circuit element $(Q_{\text{S-E}}\ (R_{\text{S-E}}\ W_{\text{S-E}}))\ R_{\text{E}}$ corresponds to the electrochemical reaction occurring between the soil sample and electrode. This circuit element is not considered because it has nothing to do with the microstructure of the soil sample and the conductive path.

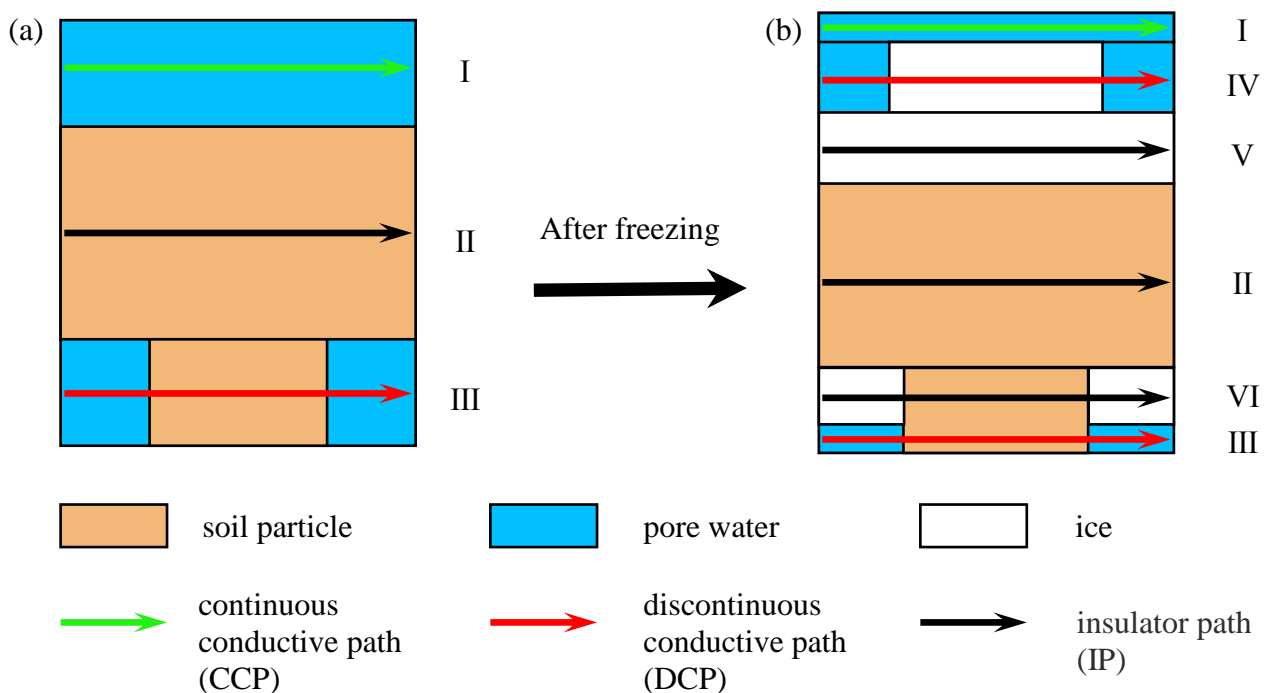### 3.3.2. Equivalent circuit model and impedance (Z_S) for sandy soil

Figure 6. The simplified microstructure of sandy soil: (a) above the freezing temperature, and (b) below the freezing temperature. The green, black, and red lines represent continuous conductive paths (CCPs), discontinuous conductive paths (DCPs), and insulating paths (IPs), respectively.

According to some studies [8, 9, 25-29], the microstructure of saturated sandy soil can be simplified as shown in Figure 6, where the orange areas represent soil particles, the blue areas represent pore water, and the white areas stand for ice. The porosity of the soil sample can be expressed by the ratio of the blue areas over the whole block (blue areas + black areas) in Figure 6.

When the saturated soil sample temperature is above the freezing temperature, it consists of soil particles and pore water [30]. Thus, there are three kinds of conductive paths, as shown in Figure 6(a): continuous pore water conductive paths (Path I), continuous soil particle conductive paths (Path II) and continuous soil particle-pore water conductive paths (Path III); when the saturated soil sample is

cooled below the freezing temperature, some pore water transforms to ice, but there is always some unfrozen water [28]. So, the soil sample is composed of three different constituents: solid particles, ice and liquid water [16, 28]. Thus, three new conductive paths are formed in the saturated freezing soil, and there are continuous pore water-ice conductive paths (Path IV), continuous ice conductive paths (Path V) and continuous soil particle-ice conductive paths (Path VI), as shown in Figure 6(b). Path I can be treated as a continuous conductive path (CCP). The silica content of the ISO standard sand used in this study is 98.7%, and hence, the soil particles can be considered as insulators. Similarly, the ice formed when part of the pore water freezes is also an insulator. So, Path III and Path IV can be treated as discontinuous conductive paths (DCPs). Soil particles and ice are considered as discontinuous points. Path II, Path V and Path VI can act as insulating paths (IPs) [6-8].

The conductivity of a soil sample before and after freezing depends on the total impedance of these three kinds of conductive paths, which can be incorporated into an equivalent circuit model, as shown in Figure 7(a).
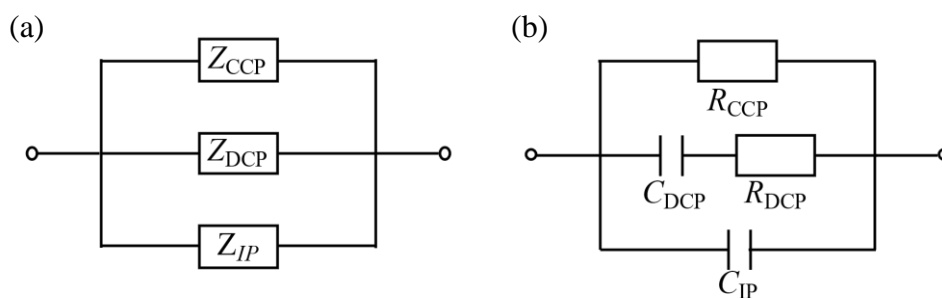

Figure 7. Equivalent circuit model for the soil sample

Correspondingly, the total impedance (Z_S) of the soil sample can be described by Equation (3):
$$Z_S = 1/(1/Z_{CCP}+1/Z_{DCP} +1/Z_{IP}) \tag{3}$$
where Z_S is the total impedance of the soil sample; Z_{CCP} is the impedance of the CCPs; Z_{DCP} is the impedance of the DCPs; and Z_{IP} is the impedance of the IPs.

The conductivity of the CCPs is through the migration of ions in pore water, Therefore, Z_{CCP} can be determined by using Ohm's law. It can be expressed as [29]:
$$Z_{CCP} = R_{CCP} \approx \rho L/S \tag{4}$$
where ρ is the resistivity of the pore water in CCP ($\Omega \cdot cm$); L is the thickness of the soil sample in the direction paralleled to the electric field (7.07 cm in this study); and S is the contact areas between the electrode and the pore water (or CCP), which is related to the water content and void ratio (e) of the soil sample (cm^2).

Due to the presence of soil particles and ice (discontinuous points) in the DCPs, the impedance (Z_{DCP}) of the DCPs consists of two parts: the impedance of the pore water in the DCPs and the impedance of the discontinuous points. The discontinuous points in the DCPs, as mentioned above, are regarded as insulators, and the AC power used in an EIS test can pass through them. So, they are like parallel plate capacitors, C_{DCP}:

$$C_{DCP} = \varepsilon_0 \left(\varepsilon_{rs} + \varepsilon_{ri} \right) S_1 / d_1 \tag{5}$$

where ε_0 is the vacuum dielectric constant (8.85×10^{-14} F/cm); ε_{rs} is the relative dielectric constant of soil particles; ε_{ri} is the relative dielectric constant of ice; S_1 is the total areas of soil particles and ice (discontinuous points) in the direction perpendicular to the electric field in DCPs (cm^2); and d_1 the cumulative thickness of the discontinuous points (cm).

Like Z_{CCP}, the impedance of the pore water in the DCPs can be expressed as R_{DCP}:

$$R_{DCP} \approx \rho (L - d_1)/S \tag{6}$$

Therefore, the impedance of the DCPs can be given by:

$$Z_{CCP} = R_{DCP} + 1/j\omega C_{DCP} \tag{7}$$

where j is the imaginary unit with $j = \sqrt{-1}$, and ω is the angular frequency.

For the insulator paths (IPs), the two end faces of the IPs in contact with the working electrode (WE) and counter electrode (CE) could serve as a parallel plate capacitor C_{IP}, and the soil particles and ice as the dielectric in the capacitor [6, 8]. Its capacitance is given by Equation (8):

$$C_{IP} = \varepsilon_0 \left(\varepsilon_{rs} + \varepsilon_{ri} \right) S_2 / L \tag{8}$$

where S_2 is the total contact areas between the IPs and the electrode (cm^2).

Therefore, the impedance of the IPs can be given by:

$$Z_{IP} = 1/j\omega C_{IP} \tag{9}$$

Thereby, the total impedance (Z_S) of the soil sample, using Equations (3), (4), (7) and (9), becomes:

$$Z_S = 1/[1/R_{CCP} + 1/(R_{DCP} + 1/j\omega C_{DCP}) + j\omega C_{IP}] \tag{10}$$

Therefore, more specifically, the EC model of the soil sample in Figure 7(a) can be described as (R_{CCP} (C_{IP} (C_{DCP} R_{DCP}))) ,which is presented in Figure 7(b). The EC model used to fit the experimental EIS data is shown in Figure 8; its circuit describing code (CDC) is (R_{CCP} (C_{IP} (C_{DCP} R_{DCP}))) (Q_{S-E} (R_{S-E} W_{S-E})) R_E:
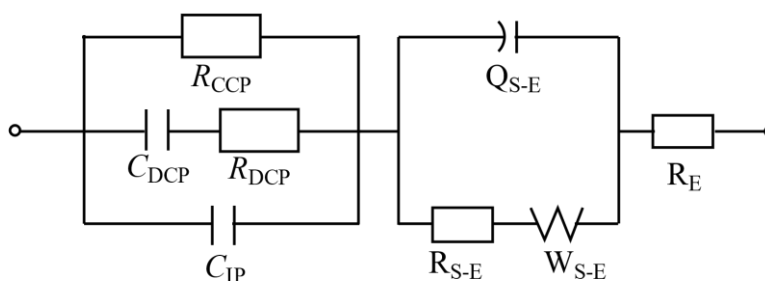

Figure 8. Equivalent circuit (EC) model used to fit experimental EIS data

3.4. Fitting results for EIS data

The EIS results are fitted using the equivalent circuit model (Figure 8) and impedance analysis software, ZSimpWin3.60. The fitting results of the EIS data for sandy soils with various NaCl contents at sub-zero temperatures are presented in Figure 3.

Int. J. Electrochem. Sci., 16 (**2021**) Article ID: 210914

12

3.4.1. Fitting verification

The degree of fitting between the measured EIS data and calculated results is evaluated by minimizing the chi-square statistic (χ^2), which is defined as the sum of the squares of the residuals [31-33], as shown in Equations (11) and (12):

$$\chi^2 = \sum_i^n \frac{\left[Z'_{msd} - Z'_{cal}\left(\omega_i\right) \right]^2 + \left[Z''_{msd} - Z''_{cal}\left(\omega_i\right) \right]^2}{\left| Z_{msd} \right|^2} \tag{11}$$

$$\left| Z_{msd} \right| = \sqrt{{Z'_{msd}}^2 + {Z''_{msd}}^2} \tag{12}$$

where n is the number of measured data points; Z'_{msd} and Z''_{msd} represent the real and imaginary parts of the measured data, respectively; $Z'_{cal}\left(\omega_i\right)$ $Z''_{cal}\left(\omega_i\right)$ represent the real and imaginary parts of the calculated results, respectively; and $\left| Z_{msd} \right|$ is the modulus of the measured data, which is used as the weighting factor to determine the optimum parameters. It is obvious that χ^2 indicates the sum of the squares of the residuals, and the smaller the value, the better the accuracy of the fitting. It is generally believed that it is acceptable when the chi-square value is less than or equal to 10^{-3} (order of magnitude). The χ^2 values for soils with different NaCl contents at sub-zero temperatures are listed in Table 4. The chi-square values between calculated results and measured data are within 10^{-4} (order of magnitude), which depicts the best fitting agreement of the equivalent circuit model (Figure 3)

Table 4. Chi-squares (χ^2) for soils with various NaCl contents at sub-zero temperatures

NaCl content	Temperature	Chi-square (χ^2)	NaCl content	Temperature	Chi-square (χ^2)
	0	2.924E-04		0	2.420E-04
	-5	2.211E-04		-5	2.505E-04
1%	-10	1.103E-04	3%	-10	3.602E-04
	-15	8.529E-05		-15	3.031E-04
	-20	1.251E-04		-20	1.842E-04
	0	1.563E-04		0	2.822E-04
	-5	5.995E-04		-5	2.790E-04
2%	-10	1.124E-04	5%	-10	3.384E-04
	-15	1.367E-04		-15	3.633E-04
	-20	7.521E-05		-20	4.134E-04

3.4.2. Calculated equivalent circuit element parameters

Table 5. Calculated values of the equivalent circuit element parameters of Z_S

NaCl content	Temperature (°C)	R_{CCP} (kΩ·cm²)	Error %	R_{DCP} (kΩ·cm²)	Error %	C_{DCP} (μF/cm²)	Error %	C_{IP} (pF/cm²)	Error %
	0	41.70	0.38	15.62	6.90	0.49	3.78	8.41E-07	9.39
	-5	70.57	0.31	23.94	9.66	0.56	7.99	0.20	7.54
1%	-10	144.10	0.21	49.27	8.61	8.49	4.05	0.94	7.11
	-15	245.70	0.18	81.22	6.67	21.00	8.41	1.60	5.12
	-20	415.10	0.21	116.60	9.95	32.99	5.56	2.21	6.05
	0	24.55	0.31	5.53	8.35	0.44	1.19	3.90E-08	8.67
	-5	28.70	0.59	8.02	6.25	0.60	2.85	2.67E-08	3.93
2%	-10	49.24	0.25	12.00	8.94	0.76	7.38	0.47	6.53
	-15	95.54	0.24	22.00	8.66	14.52	8.32	1.06	6.28
	-20	148.20	0.18	43.00	7.48	20.36	7.50	1.73	3.68
	0	17.75	0.34	3.33	7.11	0.70	3.42	2.30E-08	6.11
	-5	20.53	0.36	3.87	9.92	1.08	2.03	3.42E-07	4.92
3%	-10	24.10	0.43	6.02	7.41	2.12	3.16	2.24E-07	6.18
	-15	39.04	0.38	12.38	7.99	7.20	6.23	0.71	5.38
	-20	66.22	0.27	24.67	6.37	18.13	5.47	1.19	5.05
	0	14.13	0.36	2.17	4.63	0.35	1.21	1.85E-08	5.84
	-5	16.41	0.37	2.70	6.35	0.38	5.31	1.72E-08	8.14
5%	-10	19.85	0.41	4.44	7.37	0.65	4.47	1.77E-08	7.63
	-15	24.17	0.41	6.60	9.92	1.09	5.33	1.33E-08	2.23
	-20	28.76	0.42	10.50	7.23	1.25	2.91	1.26E-08	4.78

Note that the units of the C_{DCP} and C_{IP} are different.

In addition to the chi-square statistic (χ^2), another important criterion for evaluating an equivalent circuit is the fitting error of the calculated equivalent circuit element parameters. They are listed in Table 5. The parameters providing the best fit to a model have a smaller fitting error. These fitting results are reliable since all the fitting errors are less than 10%. R_{CCP} is always greater than R_{DCP} at the same temperature and NaCl content, which is consistent with the conclusion obtained by comparing Equations (4) and (6). Similarly, C_{DCP} is much greater than R_{IP} in Table 5. (Note that the units of C_{DCP} and C_{IP} are different).

(a) R_{CCP}

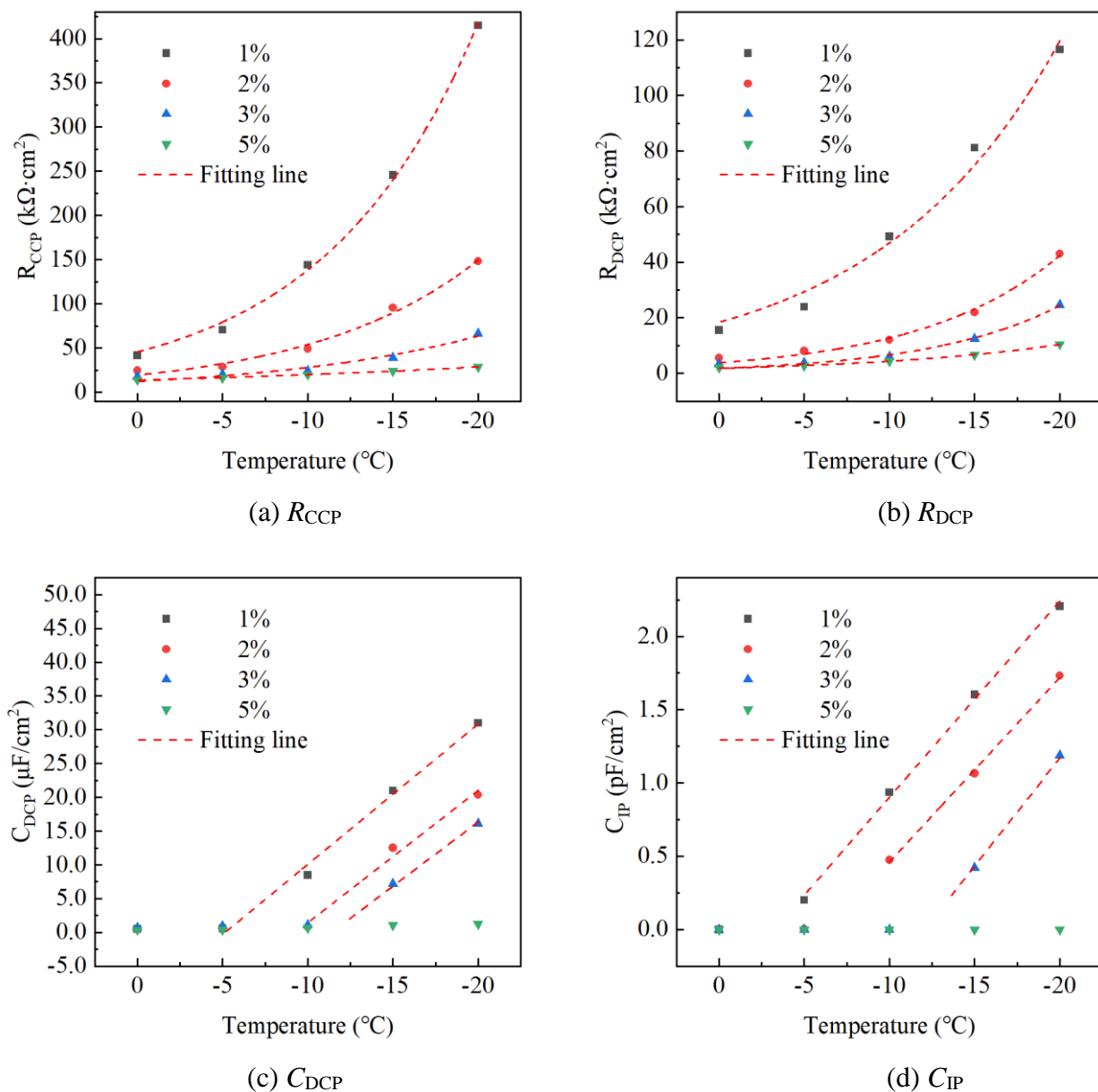(b) R_{DCP}

(c) C_{DCP}

(d) C_{IP}

Figure 9. Evolution of the calculated equivalent circuit element parameters at various NaCl contents and temperatures

In Equations (5) and (8), the ratio of S_1 and S_2 can be approximated as the void ratio e (the ratio of the volume of voids to the volume of soil solids in the soil), i.e.,

$$S_1/S_2 \approx e \tag{13}$$

And it is certain that d_1 is much smaller than L due to the porosity of the soil sample [6, 8], i.e.,

$$d_1 << L \tag{14}$$

So, the following relationship can be deduced from Equations (5), (8),(13) and (14),

$$C_{DCP} = \varepsilon_0 \left(\varepsilon_{rs} + \varepsilon_{ri} \right) \frac{S_1}{d_1} \approx \varepsilon_0 \left(\varepsilon_{rs} + \varepsilon_{ri} \right) \frac{eS_2}{d_1} \qquad C_{IP} = \varepsilon_0 \left(\varepsilon_{rs} + \varepsilon_{ri} \right) \frac{S_2}{L} \tag{15}$$

To depict the calculated equivalent circuit element parameters more intuitively, the evolution of calculated equivalent circuit element parameters (R_{CCP}, R_{DCP}, C_{DCP} and C_{IP}) at various temperatures are shown in Figure 9. R_{CCP} and R_{DCP} increase exponentially as the temperature decreases at different NaCl

contents. R_{CCP} and R_{DCP} are closely related to the pore water content in the soil sample. When the temperature is below the freezing temperature, part of the pore water in the soil sample freezes, resulting in the decrease in the unfrozen water content and the increase in R_{CCP} and R_{DCP}. The ionic conductivity of the pore water mainly depends on the migration rates of ions (Na^+ and Cl^-). The migration rates decrease with decreasing temperature; therefore, R_{CCP} and R_{DCP} increase. The functional relation can be described by the following equation:

$$R = a_1\exp(b_1 T) \tag{16}$$

where R is the resistivity of R_{CCP} or R_{DCP} ($k\Omega \cdot cm^2$); T is the temperature (°C); and a_1 and b_1 are the fitting parameters related to NaCl content and unfrozen water content.

The fitting parameters a_1 and b_1 for various NaCl contents are listed in Table 6.

Table 6. The fitting parameters a_1 and b_1 for various NaCl contents

Element	NaCl content	a_1	b_1	R^2
R_{CCP}	1%	41.76	-0.11	0.99
	2%	24.54	-0.10	0.98
	3%	17.71	-0.82	0.97
	5%	13.88	-0.36	0.98
R_{DCP}	1%	15.42	-0.09	0.98
	2%	5.43	-0.12	0.99
	3%	3.23	-0.13	0.98
	5%	2.17	-0.86	0.99

Figure 9 (c) and (d) show the trends of the capacitance of the DCPs and IPs. C_{DCP} and C_{IP} are almost invariable when the soil temperature is above the freezing temperature. Nevertheless, when the soil temperature is below the freezing temperature, C_{DCP} and C_{IP} show a significant linear increase due to the freezing of some pore water to ice. The turning point in the plots of C_{DCP} and C_{IP} provide information about the freezing temperature. The functional relationship between C_{DCP} or C_{IP} and the temperature can be described by Equation (17):

$$C = \begin{cases} C_0 & T \geq T_F \\ a_2 + b_2\left(T - T_F\right) & T < T_F \end{cases} \tag{17}$$

where C is the capacitance of C_{DCP} ($\mu F/cm^2$) or C_{DIP} (pF/cm^2); C_0 is the capacitance of the DCPs or IPs above the freezing temperature, which is a constant for a given soil in this study; C_0 is approximately equal to 1 $\mu F/cm2$ and 10^{-8} pF/cm^2 for C_{DCP} and C_{IP}, respectively; T is the temperature (°C); T_F is the freezing temperature (see

Table 3); and a_2 and b_2 are the fitting parameters related to NaCl content and unfrozen water

content, respectively.

The fitting parameters a_2 and b_2 for various NaCl contents are listed in Table 7. In this study, C_{DCP} and C_{IP} are almost invariable for the soil samples with 5% NaCl content due to the narrow temperature range. Therefore, the parameters are not listed in Table 7.

Table 7. The fitting parameters for soils with various NaCl contents

Element	NaCl content	a_2	b_2	R^2
	1%	-0.73	-2.08	0.98
C_{DCP}	2%	-0.73	-1.96	0.97
	3%	6.82	-1.99	0.99
	1%	0.21	-0.13	0.99
C_{IP}	2%	0.32	-0.13	0.98
	3%	0.24	-0.15	0.99

4. CONCLUSIONS

Electrochemical impedance spectroscopy (EIS) and an equivalent circuit (EC) model of NaCl-saturated sandy soil at sub-zero temperatures have been studied. The following conclusions can be drawn:

(1) EIS of NaCl-saturated sandy soil at sub-zero temperatures are composed of a single capacitive reactance loop and two time constants. The radius of the capacitive reactance loop and the impedance modulus increase with increasing temperature. In addition, as the temperature drops below the freezing temperature, the peak value of the maximum phase angle decreases and shifts to lower frequencies.

(2) The EC model of NaCl-saturated sandy soil at sub-zero temperatures is established on the basis of three kinds of conductive paths by analysing the microstructure of saturated sandy soil. The circuit describing code (CDC) is $(R_{CCP} (C_{IP} (C_{DCP} R_{DCP})))$, where each parameter has a physical meaning. Smaller value of the chi-square statistic (χ^2) and fitting error indicate the correctness and suitability of the equivalent circuit model, which can be used to effectively interpret the EIS results and support further studies.

(3) The fitting results show that the values of R_{CCP} and R_{DCP} at different NaCl contents increase exponentially with decreasing temperature due to the decrease in unfrozen pore water content and the migration rates of ions (Na^+ and Cl^-). There is an obvious change from almost constant values of C_{DCP} and C_{IP} to significant increasing linear trends. This change in turning point depends on the freezing temperature and can be explained by the freezing of water to ice.

Int. J. Electrochem. Sci., 16 **(2021)** Article ID: 210914

17

References

1. C. Lyu, Q. Sun, W.Q. Zhang and S. Q. Hao, *J. Appl. Geophys.*, 170 (2019) 103843.
2. T. T. X. Hang, T. A. Truc, T. H. Nam, V. K. Oanh, J. Jorcin and N. Pebere, *Surf. Coat. Technol.*, 201 (2008) 7408.
3. M. C. Yan, C. Sun, J. Xu, J. H. Dong and W. Ke, *Corros. Sci.*, 80 (2014) 309.
4. M. C. Yan, C. Sun, J. H. Dong, J. Xu and W. Ke, *Corros. Sci.*, 97 (2015) 62.
5. E. Joanna, T. Hisasi, A. S. Bachir and T. Said, *Corros. Sci.*, 168 (2020) 108556.
6. G. L. Song, *Cement Concrete Res.*, 30 (2000) 1723.
7. M. Jin, L.H. Jiang, M.T. Lu, N. Xu and Q. Zhu, *Constr. Build. Mater.*, 152 (2017) 702.
8. P. J. Han, Y. F. Zhang, F. Y. Chen and X. H. Bai, *J. Cent. South Univ.*, 22 (2015) 4318.
9. R. Z. Xie, P. J. Han, X. Y. Wang, B. Q. Li, B. He, F. L. Ma, X. H. Bai, *Int. J. Electrochem. Sci.*, 15 (2020) 3543.
10. K. Belmokre, N. Azzouz, F. Kermiche, M. Wery and J. Pagetti, *Mater. Corros.*, 49 (1998) 108.
11. M. Behzadnasab, S. M. Mirabedini and M. Esfandeh, *Corros. Sci.*, 75 (2013) 134.
12. L. M. Quej-Ak, M. J., R. G. N-Cruz, N-Mart and A. C. Nez, *Mater. Sci. Forum*, 793 (2014) 169.
13. P. J. Han, R. Z. Xie, N. M. Lin and B. He, *Int. J. Electrochem. Sci.*, 11 (2016) 9491.
14. X. Wei, Y. M. Liu, J. H. Dong, S. F. Cao, J. L. Xie, N. Chen, F. Xue, C. G. Wang and W. Ke, *Appl. Clay Sci.*, 167 (2019) 23.
15. S. Q. Peng, F. Wang and L. Fan, *Int. J. Electrochem. Sci.*, 14 (2019) 8611.
16. O. B. Andersland and B. Ladanyi, Mechanical Properties of Frozen Soils, *Springer*, (1994) Boston, U.S.A..
17. X. S. Wan, Y. M. Lai and C. Wang, *Permafrost Periglac.*, 26 (2015) 175.
18. Q. L. Xie and W. M. Chen, *Corros. Sci.*, 86 (2014) 252.
19. S. L. D. Assis, S. Wolynec and I. Costa, *Electrochim. Acta*, 51 (2006) 1815.
20. Z. B. Wang, H. X. Hu, C. B. Liu and Y. G. Zheng, *Electrochim. Acta*, 135 (2014) 526.
21. J. E. G. González and J. C. Mirza-Rosca, *J. Electroanal. Chem.*, 471 (1999) 109.
22. A. Lasia, Electrochemical Impedance Spectroscopy and its Applications, *Springer*, (2014) New York, U.S.A..
23. S. Tamilselvi, V. Raman and N. Rajendran, *Electrochim. Acta*, 52 (2006) 839.
24. Y. F. Lu, J. H. Dong and W. Ke, *J. Mater. Sci. Technol.*, 31 (2015) 1047.
25. Á. N. Bhreasail, P. D. Lee, C. O'Sullivan, C. H. Fenton, R. Hamilton, P. Rockett and T. Connolley, *Permafrost Periglac.*, 23 (2012) 170.
26. G. C. Sun, J. M. Zhang, Y. S. Dang and C. Ding, *J. Mt. Sci.-Engl.*, 16 (2019) 1470.
27. K. Xue, Z. Wen, X. H. Ma, M. L. Zhang, Q. Gao and N. Sun, *J. Glaciol. Geocryol.*, 41 (2019) 1122.
28. X. D. Zhang, Q. Wang, G. Wang, W. H. Wang, H. E. Chen and Z. Q. Zhang, *Math. Probl. Eng.*, 2017 (2017) 1.
29. L.Y. Tang, K. Wang, L. Jin, G. S.Yang, H.L. Jia and A. Taoum, *Cold Reg. Sci. Technol.*, 153 (2018) 55.
30. R. Kido, Y. Higo, F. Takamura, R. Morishita, G. Khaddour and S. Salager, *Acta Geotech.*, 15 (2020) 1745.
31. X. H. Zhang, S. O. Pehkonen, N. Kocherginsky and G. Andrew Ellis, *Corros. Sci.*, 44 (2002) 2507.
32. S. Surviliene, A. Lisowska-Oleksiak and A. Česuniene, *Corros. Sci.*, 50 (2008) 338.

33. G. J. Liu, Y. S. Zhang, M. Wu and R. Huang, *Constr. Build. Mater.*, 157 (2017) 357.